Phononic and electronic Raman spectroscopy of the pseudogap state in underdoped $YBa_2Cu_3O_{7-x}$

M. F. Limonov* and S. Tajima
Superconductivity Research Laboratory, ISTEC, Shinonome 1-10-13, Koto-ku, Tokyo 135-0062, Japan

A. Yamanaka
Chitose Institute of Science and Technology, Chitose, Hokkaido 066-8655, Japan
(Received 23 February 2000; revised manuscript received 21 July 2000)

Electronic and phononic Raman scattering spectra have been studied in detwinned crystals of underdoped $YBa_2Cu_3O_{7-x}$ with $T_c=63$ K. In contrast to a very weak response of the B_{1g} spectrum at all temperatures, we found at $T<180$ K a strong suppression of the electronic Raman scattering with A_{1g} symmetry below 700 cm^{-1} and remarkable self-energy effects on the A_{1g} phonon at 120 cm^{-1}. Both phenomena are indicative of a gradual decrease in the electronic response, resulting from a pseudogap that opens on a large area of the Fermi surface. Superconductivity-induced phonon renormalization can be observed strongly in the A_{1g} and weakly in the B_{1g} spectra.

I. INTRODUCTION

One of the most important problems in the study of high-T_c superconductors (HTSC's) is an origin of the pseudogap that appears well above T_c in the underdoped regime. Although a huge number of experimental results have been accumulated,[1] the relationship between the pseudogap and superconductivity is still an open question. Recent results of angle-resolved photoemission spectroscopy (ARPES) (Ref. 2) revealed that a pseudogap gradually opens with lowering temperature (T), depending on $\mathbf{k}$, namely, that the pseudogap opens first at the Fermi surface around $[\pi,0]$ and $[0,\pi]$ and then widens towards $[\pi/2,\pi/2]$ direction. In order to understand the apparently controversial situation that the pseudogap is observed at different temperatures in different physical properties, the $\mathbf{k}$ dependence of the pseudogap is extremely important. Except for ARPES, there are only a few experimental probes for the $\mathbf{k}$ dependence of the Fermi surface. Raman scattering spectroscopy is one of the promising tools that can determine the $\mathbf{k}$ dependence of a gap magnitude. In fact, in the study of superconducting gap symmetry, the Raman results have played an important role.[3] Compared with ARPES, a Raman spectrum is less sensitive to a sample surface, which enables us to investigate not only the cleavages of $Bi_2Sr_2CaCu_2O_8$ but also other HTSC's such as $YBa_2Cu_3O_{7-x}$.

There have been several reports of electronic Raman studies for the pseudogap.[4–9] In contrast to the case of the highly doped regime, almost no T dependence was observed in the B_{1g} spectrum of the underdoped crystals, while the B_{2g} spectrum shows suppression of a spectral weight below 700 cm^{-1} at low temperatures.[7,8] Since the B_{1g} and B_{2g} spectra detect mainly the electronic states of the Fermi surface near $[\pi,0]$ and $[\pi/2,\pi/2]$, respectively, the above results seem to be contradictory to the other reports that suggest a d-wave symmetry of the pseudogap[2] and motivates us to investigate other symmetry spectra such as A_{1g} to probe the whole Fermi surface.

On the other hand, the electronic change should affect the phonon self-energy $\Sigma=\Sigma'+i\Sigma''$, i.e., its frequency $\omega=\omega_0-\Sigma'$ and linewidth $2\Gamma=2(\Gamma_0+\Sigma'')$, through the $\mathbf{k}$-dependent electron-phonon interaction $g(\mathbf{k})$. An advantage of phonon Raman scattering study is that it can measure both the real and imaginary parts of the electronic response through Σ, whereas the electronic Raman scattering only measures the imaginary part. Thus the phonon self-energy Σ provides complementary and crucial information for the pseudogap. However, so far there has been little reports on the phonon Raman study of the pseudogap problem.

The polarized Raman spectra probes different parts of the Fermi surface and therefore can provide information on anisotropies of both pseudogap and superconducting gap. In this paper we refer to a tetragonal D_{4h} point group with X and Y taken parallel to the Cu-O bonds. The B_{1g} ($X'Y'$) Raman spectra samples the Fermi surface near the $(0,\pm1)$ and $(\pm1,0)$ directions in the Brillouin zone whereas the B_{2g} (XY) spectrum samples a region near the $(\pm1,\pm1)$ diagonals. The A_{1g} channel is more isotropic and samples the Fermi surface both near the $(0,\pm1)$, $(\pm1,0)$, and near the $(\pm1,\pm1)$ directions. In contrast to B_{1g} and B_{2g} channels, the A_{1g} channel cannot be individually measured by in-plane scattering geometries and one measures a combination of A_{1g} and either B_{1g} (XX,YY) or B_{2g} ($X'X'$,$Y'Y'$) components.[3] Although we measured spectra with various polarization configurations, we focus our discussion here on the XX- and YY-polarization spectra with the $(A_{1g}+B_{1g})$ symmetry, which is complementary to the well investigated B_{2g} symmetry. Taking an advantage of the phonon-rich spectrum with A_{1g} symmetry in $YBa_2Cu_3O_{7-x}$, we also extract information on the electronic state through the phonons.

II. EXPERIMENT

The $YBa_2Cu_3O_{7-x}$ crystals were grown by a top-seeded pulling technique and oxygenated under uniaxial pressure in order to make twin-free samples.[10] By controlling the post-annealing temperature in flowing oxygen, we prepared an underdoped crystal with $T_c=63$ K and an optimally doped crystal with $T_c=93$ K. We refer to the former as UndD and to the latter as OptD hereafter.

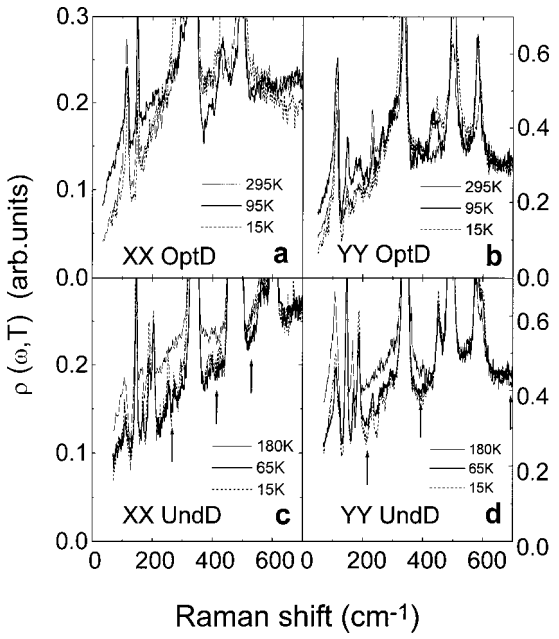

FIG. 1. The Raman response functions $\rho(\omega)$ for the *XX* and *YY* scattering geometries of the OptD crystal (a) and (b) and the UndD crystal with $T_c = 63$ K (c) and (d) at different temperatures.

The Raman scattering spectra were measured in the pseudobackscattering configuration with the 514.5-nm line of an Ar-Kr^+ laser, using a triple stage spectrometer with a liquid-nitrogen-cooled charge-coupled device (CCD) detector. A typical spectral resolution was 3 cm^{-1}. The laser power density was about 5 W/cm^2 on the sample surface, and the overheating was estimated from Stokes-Antistokes ratio to be less than 10 K. For low-*T* measurements, a closed-cycle cryostat was used with temperature stabilization better than 1 K. All the measurement temperatures are corrected for the laser heating.

III. RESULTS AND DISCUSSION

Temperature-dependent Raman spectra of the OptD and UndD samples are shown in Fig. 1. The contribution of the Bose factor has been removed, so that the spectrum is proportional to the imaginary part of the Raman scattering response function $\chi(\omega) = R(\omega) + i\rho(\omega)$. At room temperature, all spectra consist of rather flat electronic continuum and superimposed by five well known phonon lines at about 120, 150, 340, 430, and 500 cm^{-1}. Additionally, the *YY*-polarized spectra are modified by defect phonon modes, since oxygen defects are mainly formed in the CuO chains along the *Y* axis. Figure 1 shows that the temperature dependence of $\rho(\omega)$ is quite different between OptD and UndD crystals. As for OptD the low-ω electronic continuum slightly increases with lowering *T* down to T_c, arising from the *T* dependence of the electronic scattering rate $\Gamma_e(\omega)$.[11] Below T_c the spectrum exhibits a superconducting response with a broad peak which reflects the **k** dependence of a $d_{x^2-y^2}$ paring state.[3,12] In contrast, for UndD the electronic continuum at $\omega < 700\,cm^{-1}$ is anomalously suppressed in the *XX* and *YY* spectra at temperatures well above T_c but it is less sensitive to *T* below T_c. The normal-state anomaly in UndD is considered to be due to opening of the pseudogap. As is shown in Figs. 1(a) and 1(b), there is no evidence for a pseudogap in the spectrum for OptD.

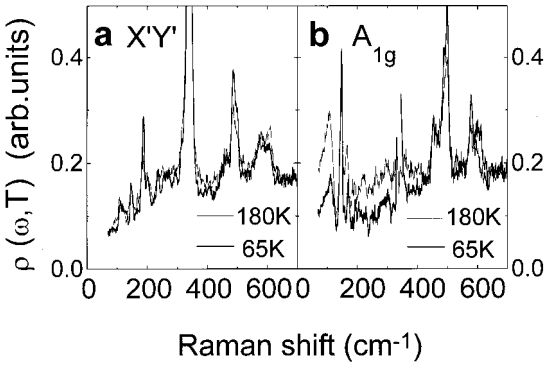

FIG. 2. (a) The Raman response functions $\rho(\omega)$ for the $X'Y'$ scattering geometry of the UndD crystal with $T_c = 63$ K at different temperatures. (b) The A_{1g} component calculated from Figs. 1(c) and 1(d) and 2(a) as $I(A_{1g}) = [I(XX) + I(YY)]/2 - I(X'Y')$.

The $X'Y'$ spectra with B_{1g} symmetry are shown in Fig. 2(a). Since temperature dependence of the B_{1g} spectra is very weak above T_c, the observed change in the *XX* and *YY* spectra is attributed to the *T* dependence of the A_{1g} spectra. In fact, the A_{1g} component [Fig. 2(b)] calculated from Figs. 1(c) and 1(d) and 2(a) as $I(A_{1g}) = [I(XX) + I(YY)]/2 - I(X'Y')$ shows a remarkable suppression above T_c.

Figure 3 shows *T* dependencies of the electronic intensities at several frequencies, marked by the arrows in Figs. 1(c) and 1(d). The suppression occurs at $T^* \sim 180$ K, which agrees well with the pseudogap anomaly detected by tunneling measurements.[13,14] Since no significant *T* dependence is observed in the B_{1g} channel, the observed *T* dependence in Fig. 3 must originate from the A_{1g} channel, as is shown in Fig. 2. A spectral weight reduction for the A_{1g} part is estimated to be about 40% at 200 cm^{-1}. As for the *YY* spectrum, the continuum partly originates from the chains. However, the amount of the reduction in the *YY* is nearly the same as that in the *XX*, indicating that a pseudogap does not open in the chain band.

Next let us consider the phonon spectrum which reflects the real and imaginary parts of the electronic response χ through the phonon self-energy $\Sigma = \Sigma' + i\Sigma''$.[15] Among various phonons in $YBa_2Cu_3O_{7-x}$, we focus our attention on the Ba-vibration phonon with A_{1g} symmetry at about 120 cm^{-1}, because this phonon has been found to couple strikingly with the A_{1g} electronic continuum. Thus we expect the self-energy effect on this phonon to be mainly related to the electronic excitations. A possibility of strong electron-phonon coupling for the A_{1g} Ba mode was also predicted by the linearized-augmented-plane-wave calculation.[16] As clearly shown in Fig. 4, strong coupling of the 120-cm^{-1} phonon with the electronic continuum gives rise to the quantum interference, resulting in an asymmetric line shape. With decreasing *T*, this phonon peak shifts towards high frequency below 150 K and goes back at $T < T_c$. The linewidth and the intensity also show a similar *T* dependence. By contrast to this complicated behavior of the Ba mode, the Cu-vibration mode at 147 cm^{-1} exhibits no appreciable *T* dependence. This indicates that the latter phonon hardly couples with the electronic continuum.

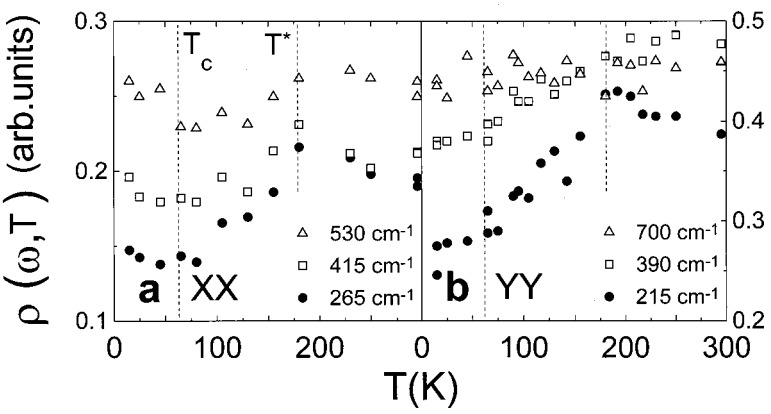

FIG. 3. Temperature dependencies of the Raman response functions $\rho(\omega)$ in the *XX* and *YY* polarizations for the UndD crystal ($T_c = 63$ K) at the frequencies ω indicated by the arrows in Figs. 1(c) and 1(d).

To estimate the self-energy Σ by removing the interference, we have fitted the spectrum with the Fano formula.[12,17,18] The fitting result is illustrated by the solid lines in Fig. 4. A Lorentzian line shape is assumed for the Cu phonon at 147 cm^{-1} and for a defect phonon mode that appears as a shoulder at about 125 cm^{-1}. Temperature dependencies of the frequency and the linewidth of the 120-cm^{-1} mode are plotted in Fig. 5, where the results for OptD are shown for comparison. The solid lines display the T dependencies expected from the two-phonon decay process.[19,20] In the behavior of the 120-cm^{-1} mode, we immediately see opening of the pseudogap at $T^* \sim 150$ K and the superconducting gap at $T_c \sim 60$ K. The former causes hardening of the phonon frequency and narrowing of the linewidth, which correspond to decreases of the real part Σ' and imaginary part Σ'', respectively. This is consistent with the T dependence of the electronic response shown in Figs. 1–3. Note that T^* observed in the phonon parameters is slightly lower than $T^* \sim 180$ K determined from the electronic intensity at frequencies above 200 cm^{-1}. The lower phonon T^* may imply that the pseudogap effect is delayed for the phonon at a low frequency. Softening and broadening below T_c illustrates the increase of Σ' and Σ'', respectively, while this mode shows narrowing for OptD, indicating a decrease in Σ''. Later we discuss the superconductivity-induced effects in more detail.

The suppression of Σ'' below T^* results from closing a part of the decay channels owing to opening of the pseudogap. This pseudogap-induced effect is apparently similar to the superconductivity-induced narrowing that is observed in OptD. However, the physics behind them are substantially different. Namely, in the case that the bare phonon frequency ω_0 is well below $2\Delta_{max}$ for a *d*-wave superconducting gap, the imaginary part Σ'' decreases with lowering T, because thermally excited quasiparticles become frozen out. The low-T Σ'' is associated with creation process of the quasiparticle pairs above a smaller gap $[2\Delta(\mathbf{k}) < \omega_0]$ near the nodes.

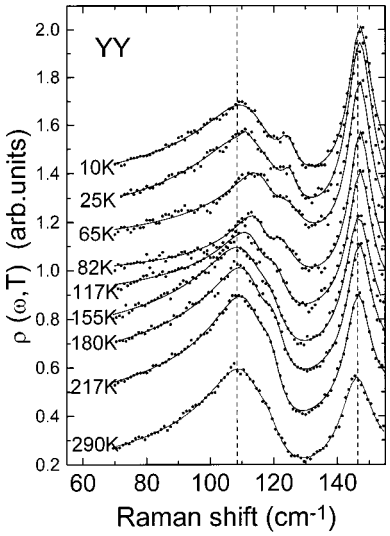

FIG. 4. Temperature dependencies of the Raman response functions $\rho(\omega)$ for UndD $YBa_2Cu_3O_{7-x}$ crystals for the *YY* scattering geometry. All solid lines are the fitting results by the Fano approach. Each spectrum is shifted vertically by 0.15 from the previous one.

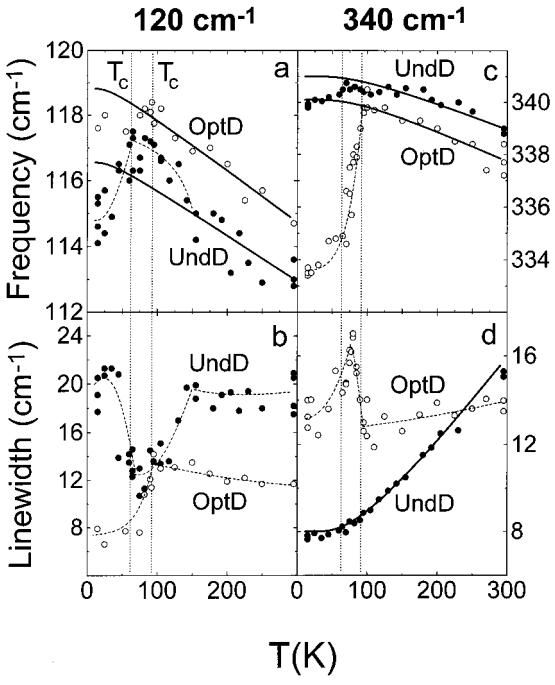

FIG. 5. Temperature dependencies of the fitting parameters of the 120 and 340 cm^{-1} phonon lines for the OptD (open circles) and UndD (solid circles) $YBa_2Cu_3O_{7-x}$ crystals. (a) and (c) Renormalized phonon frequencies $\Omega = \Omega_0 + \Sigma'$. (b) and (d) Renormalized phonon linewidths $2\Gamma = 2(\Gamma_0 + \Sigma'')$. The solid lines are the expected curves in the two phonon decay model (Ref. 19). The dashed lines are guides to the eye only.

Although the pair creation in the larger gap region [$2\Delta(\mathbf{k}) > \omega_0$] cannot contribute to Σ'', this process enlarges the real part Σ', since the superconducting carriers still couple to the relevant phonons. Indeed, the softening of the 120-cm^{-1} phonon in OptD demonstrates that Σ' is enhanced in the superconducting state. On the other hand, the pseudogap-induced hardening and narrowing suggest that carriers in the pseudogap state do not contribute to the phonon self-energy Σ, as if these carriers lost their electron-phonon coupling. In this case, the residual self-energy $\Sigma_{\rm res}$ is related to the conducting carriers on the Fermi surface that survive in the pseudogap state. By assuming $2\Gamma_0=0$, the amount of $\Sigma''_{\rm res}$ is estimated to be $\Sigma''_{\rm res}/\Sigma'' = 2\Gamma(65\,{\rm K})/2\Gamma(150\,{\rm K})=0.6$. Since $2\Gamma_0\neq 0$ in an actual system, the amount would be a little smaller than 0.6.

Since the A_{1g} scattering probes the Fermi surface in the $[\pi,0]$ direction as well as $[\pi,\pi]$, it is of great interest to see the pure B_{1g} Raman response. As to the electronic Raman response at B_{1g}, no significant anomaly related to the pseudogap or superconducting gap is observed in the underdoped HTSCs. As a more sensitive probe, we have used the self-energy effect on the well-known B_{1g} phonon at about 340 cm^{-1}. The results are shown in Figs. 5(c) and 5(d) as solid circles. The linewidth follows well the T dependence of phonon-phonon scattering over the whole T range. The frequency shows weak softening at T_c but the pseudogap is indistinguishable. We conclude that carriers for B_{1g} are already suppressed or almost incoherent at room temperature. This possibility has been pointed out by the photoemission experiments on $Bi_2Sr_2CaCu_2O_{8+z}$, which have revealed a remarkable loss of the density of states at E_F in the UndD regime, extending to a large energy scale with an order of 0.1 eV.[2] Therefore it is reasonable to attribute the depletion of the B_{1g} response to the large suppression of the density of states around $[\pi,0]$. In this scenario the A_{1g} response observed in the present work does not originate from the electronic state in the $[\pi,0]$ direction but primarily from the $[\pi,\pi]$, which is the same direction as that measured at B_{2g}. Indeed, the residual $\Sigma''_{\rm res}/\Sigma''\sim 0.5$ is not very different from the residual electronic intensity $\rho_{\rm res}/\rho\sim 0.65$ for B_{2g}.[8]

Finally, we discuss the superconducting gap in the underdoped regime. As can be seen in Fig. 5, the superconductivity-induced effect on the 120-cm^{-1} phonon abruptly appears below T_c. This demonstrates that the residual carriers along the $[\pi,\pi]$ direction exhibits a striking superconducting response. The linewidth steeply increases and recovers to the normal value above T^*, while the frequency softens below T_c. These phonon behaviors suggest a gap value $2\Delta_{A1g}$ is not far from 120 cm^{-1} for A_{1g}. On the other hand, the softening of the 340 cm^{-1} indicates $2\Delta_{B1g} > 340\,{\rm cm}^{-1}$. The polarization dependence ($\Delta_{A1g}<\Delta_{B1g}$) is consistent with the theoretical prediction for a $d_{x^2-y^2}$ pairing state.[3] In sharp contrast to the phonon behavior, a superconducting response in the *XX* and *YY* electronic continuum can be hardly seen in Figs. 1 and 3. This might result from a screening effect in the A_{1g} electronic response, as was discussed by Devereaux and Einzel,[3] while the A_{1g} phonon is almost unscreened.

Concerning the gap maximum, the phonon Raman spectrum in the resonant condition for $YBa_2Cu_3O_{7-x}$ with $T_c = 70$ K suggested $2\Delta_{\rm max}>500\,{\rm cm}^{-1}$.[21,22] This value is comparable to the energy scale of the Raman pseudogap $600-800\,{\rm cm}^{-1}$, but is quite different from $2\Delta_{\rm max}\sim 8kT_c = 330\,{\rm cm}^{-1}$ expected from a sharp gap peak in the B_{2g} electronic spectrum.[7,8] A key to solve this puzzle might be a loss of coherency of carriers in the superconducting phase, which makes the gap behavior deviated from that of a clean *d* wave. Although the Fermi surface along the $[\pi,0]$ gives a large gap (>600 cm^{-1}), it is expected that many of the carriers are incoherent and do not contribute to the phonon self-energy at $T<T^*$, even below T_c, resulting in very weak softening of the B_{1g} phonon for UndD that is less than 20% of that for OptD. Only the carriers along the $[\pi,\pi]$ show the coherent superconducting response, giving a smaller gap of about 200 cm^{-1} at A_{1g} and B_{2g} channels.

IV. CONCLUSIONS

We found remarkable suppression of the A_{1g}-electronic Raman intensity below 700 cm^{-1} at $T<180$ K, accompanied by the strong self-energy effects on the A_{1g} phonon at 120 cm^{-1}. This can be attributed to opening of the pseudogap on the Fermi surface, where the carrier response for B_{1g} is already suppressed or incoherent at room temperature. The 120-cm^{-1} phonon also shows a pronounced self-energy effects below T_c, indicating that a superconducting gap opens on the residual Fermi surface.

ACKNOWLEDGMENTS

The authors thank A. I. Rykov and T. Masui for preparing the samples as well as A. G. Panfilov and J. Quilty for helpful discussions. This work was supported by New Energy and Industrial Technology Development Organization (NEDO) as Collaborative Research and Development of Fundamental Technologies for Superconductivity Applications.

*Permanent address: A. F. Ioffe Physical-Technical Institute, 194021 St. Petersburg, Russia.

[1] For a review, see T. Timusk and B. W. Statt, Rep. Prog. Phys. **62**, 61 (1999).

[2] H. Ding, T. Yokoya, J. C. Campuzano, T. Takahashi, M. Randeria, M. R. Norman, T. Mochiku, K. Kadowaki, and J. Giapintzakis, Nature (London) **382**, 51 (1996); A. G. Loeser, Z.-X. Shen, D. S. Dessau, D. S. Marshall, C. H. Park, P. Fournier, and A. Kapitulnik, Science **273**, 325 (1996).

[3] T. P. Devereaux, D. Einzel, B. Stadlober, R. Hackl, D. H. Leach, and J. J. Neumeier, Phys. Rev. Lett. **72**, 396 (1994); T. P. Devereaux and D. Einzel, Phys. Rev. B **51**, 16 336 (1995).

[4] F. Slakey, M. V. Klein, J. P. Rice, and D. M. Ginsberg, Phys. Rev. B **42**, 2643 (1990).

[5] G. Blumberg, M. Kang, M. V. Klein, K. Kadowaki, and C. Kendziora, Science **278**, 1427 (1997).

[6] X. K. Chen, J. G. Naeini, K. C. Hewitt, J. C. Irwin, R. Liang, and W. N. Hardy, Phys. Rev. B **56**, R513 (1997).

[7] R. Nemetschek, M. Opel, C. Hoffmann, P. F. Müller, R. Hackl, H. Berger, L. Forro, A. Erb, and E. Walker, Phys. Rev. Lett. **78**, 4837 (1997); R. Hackl, M. Opel, P. F. Müller, G. Krug, B. Stadlober, R. Nemetschek, H. Berger, and L. Forro, J. Low

Temp. Phys. **105**, 733 (1996); M. Opel, R. Nemetschek, C. Hoffmann, R. Philipp, P. F. Müller, R. Hackl, I. Tütto, A. Erb, B. Revaz, E. Walker, H. Berger, and L. Forro, Phys. Rev. B **61**, 9752 (2000).

[8] M. Opel, M. Götzinger, C. Hoffmann, R. Nemetschek, R. Philipp, F. Venturini, R. Hackl, A. Erb, and E. Walker, J. Low Temp. Phys. **117**, 347 (1999).

[9] J. G. Naeini, X. K. Chen, J. C. Irwin, M. Okuya, T. Kimura, and K. Kishio, Phys. Rev. B **59**, 9642 (1999).

[10] A. I. Rykov, W. J. Jang, H. Unoki, and S. Tajima, in *Advances in Superconductivity VIII*, edited by H. Hayakawa and Y. Enomoto (Springer-Verlag, Tokyo, 1996), p. 341.

[11] F. Slakey, M. V. Klein, J. P. Rice, and D. M. Ginsberg, Phys. Rev. B **43**, 3764 (1991); D. Einzel and R. Hackl, J. Raman Spectrosc. **27**, 307 (1996).

[12] M. F. Limonov, A. I. Rykov, S. Tajima, and A. Yamanaka, Phys. Rev. B **61**, 12 412 (2000).

[13] M. Gurvitch, J. M. Valles, Jr., A. M. Cucolo, R. C. Dynes, J. P. Garno, L. F. Schneemeyer, and J. V. Waszczak, Phys. Rev. Lett. **63**, 1008 (1989).

[14] For a review, see T. Hasegawa, H. Ikuta, and K. Kitazava, in *Physical Properties of High Temperature Superconductors III*, edited by D. M. Ginsberg, (World Scientific, Singapore, 1992) p. 525.

[15] In general, the phonon self-energy Σ is not the direct reflection of the electronic response χ, because the $\mathbf{k}$ dependence of the electronic Raman vertex $\gamma(\mathbf{k})$ and the electron-phonon interaction $g(\mathbf{k})$ are different, and also because the screening effect that is significant in the A_{1g} scattering is different in Σ and χ.

[16] R. E. Cohen, W. E. Pickett, and H. Krakauer, Phys. Rev. Lett. **64**, 2575 (1990).

[17] C. Thomsen, in *Light Scattering in Solids VI*, edited by M. Cardona and G. Guntherodt (Springer-Verlag, Berlin, 1991).

[18] Although the interference effect can be treated more strictly by using a Green's function as we did in our previous paper (Ref. 12) it is impossible in the present case, because many defect-induced phonon lines appear in the Raman spectra of the underdoped $YBa_2Cu_3O_{7-x}$, which restricts the spectral range for analysis.

[19] The two-phonon-decay model (Ref. 20): the bare phonon frequency is described as $\Omega_0(T)=\Omega(T_0)-A[1+2n(\omega/2,T)]$, the bare linewidth as $\Gamma_0(T)=\Gamma(T_0)+B[1+2n(\omega/2,T)]$, where $n(\omega,T)=1/[\exp(\hbar\omega/k_BT)-1]$.

[20] M. Balkanski, R. F. Wallis, and E. Haro, Phys. Rev. B **28**, 1928 (1983).

[21] A. G. Panfilov, M. F. Limonov, A. I. Rykov, S. Tajima, and A. Yamanaka, Phys. Rev. B **57**, R5634 (1998).

[22] E. Altendorf, X. K. Chen, J. C. Irwin, R. Liang, and W. N. Hardy, Phys. Rev. B **47**, 8140 (1993).